

Effect of inclination angle on natural convection from inclined plate with variable viscosity and thermal conductivity

Ghassan Adnan Abid

Mechanical Engineering Department

College of Engineering

Thi-Qar University

Abstract

In this paper, a numerical investigation of a natural convection from an isothermal inclined plate immersed in air has been done. Taking into account the variation of the viscosity and thermal conductivity with temperature. The governing conservation equations of continuity, momentum and energy are non-dimensionalized by using an appropriate transformation. The non-dimensionalized equations are solved simultaneously by using a finite volume method. The effect of inclination angle with varying viscosity and thermal conductivity on the local skin friction, local Nusselt number, average skin friction and average Nusselt number has been discussed. From the results obtained the allotment of the local skin friction and the local Nusselt number on the plate vary due to angle change. The average skin friction and the average Nusselt number decrease with increase of the angle of inclination.

keyword: Natural convection, inclined plate, variable viscosity, variable conductivity

المستخلص:

تم في هذا البحث دراسة تأثير زاوية ميلان صفيحة ساخنة على الحمل الحر مع الاخذ بنظر الاعتبار تغيير كل من اللزوجة و الموصلية الحرارية مع درجة الحرارة. باستخدام التعويض المناسب تم تحويل معادلات الاستمرارية، الزخم والطاقة الى معادلات لا بعدية. تم حل المعادلات اللابعدية باستخدام طريقة الحجم المحددة. تم مناقشة تأثير زاوية ميلان الصفيحة مع تغيير اللزوجة و الموصلية الحرارية على كل من الاحتكاك السطحي الموقعي، عدد نسلت الموقعي، معدل الاحتكاك السطحي ومعدل عدد نسلت. النتائج التي تم الحصول عليها تشير الى ان توزيع كل من الاحتكاك السطحي الموقعي وعدد نسلت الموقعي على الصفيحة يتغير بتغيير زاوية الميلان. كما ان معدل الاحتكاك السطحي ومعدل عدد نسلت يقل بزيادة زاوية الميلان.

1. Introduction:

Natural convection is very common phenomenon in a number of practical applications such as solar collectors, electronic component and chemical processing equipment, it is caused by the temperature difference between the body and the fluid surrounding it that produce density difference in the fluid result in natural flow. Many literatures exist about natural convection from flat plate because of its engineering application but most of these previous studies have been conducted natural convection with constant properties for vertical or horizontal plates. Natural convection along an inclined flat plate has encountered less interest than the case of vertical or horizontal plates. Michiyoshi [1] studied heat transfer from an inclined thin plate by natural convection theoretically. The results show the local heat transfer coefficient is inversely proportional to the thickness of the boundary layer and the heat transfer coefficient of vertical plate is larger than that for inclined plate.

H.T. Lin et al [2] conducted the heat and mass transfer from a vertical plate maintained at uniform wall heat flux and species concentration by free convection. They founded correlation equations for estimating the rate of mass transfer and heat transfer.

N. Onur et al [3] conducted experimental study on the effects of inclination and plate spacing on natural convection heat transfer between parallel plates. The angles investigated are 10, 30 and 45 with respect to the vertical and for a separation distance from 2 mm to 33 mm. the lower plate isothermally heated and the upper plate thermally insulated. They found that Nusselt number depends on the separation distance between the plates. Heat transfer results also depend on plate inclination.

P. Ganesan et al [4] studied numerically the unsteady heat and mass transfer from impulsively started inclined plate. It is observed that local wall shear stress decreases as an angle of inclination decreases.

T.D. Jr et al [5] studied natural convection from vertical plate in the present of heat source. Using finite volume method to solve the governing equations describe this phenomenon. The influence of the source size on the transition region deserves more attention. The presence of this region of transition emphasizes the complexity of this kind of flow.

L.S. Yao [6] studied the natural convection along a complex vertical surface created from two sinusoidal functions. The numerical results show that the total heat transfer

rate for the wavy surface is indeed much greater than that of a flat plate. The enhanced rate is proportional to the ratio of amplitude to the wavelength of the surface.

N. C. Mahanti et al [7] studies numerically the effect of linearly varying viscosity and thermal conductivity on steady free convective flow and heat transfer along an isothermal vertical plate in the presence of heat sink. For their study the velocity and temperature of the fluid decrease with increase Prandtl number. The velocity and thermal boundary layer thickness decrease with increase Prandtl number and decrease with the decrease in the heat sink parameter.

S.C.saha et al [8] investigated the natural convection from inclined cooled plate ramp cooling condition by using scaling analysis. They show that the development of the boundary layer flow depends on the comparison of the time at which the ramp cooling is complete with the time at which the boundary layer completes its growth. The cold boundary layer is potentially unstable to the Rayleigh-Benard instability.

S. Siddiqua et al [9] investigated natural convection from a semi-infinite flat plate inclined at small angle to the horizontal with internal heat generation and exponential variation of viscosity. The governing equations are transformed into dimensionless equations which are solved using finite difference method. It is observed that as increase the inclination angle both heat transfer rate and skin friction coefficient increase. It is also shown that with an increase in heat generation, the local skin friction increase while the heat transfer rate decrease for a high Prandtl number.

G. Palani et al [10] studied numerically the unsteady natural convection from vertical plate with variable viscosity and thermal conductivity. The governing equations are solved numerically using finite difference scheme. The results show as the viscosity parameter increases the higher velocity is observed in the region near the wall and it gives higher Nusselt number and lower skin friction. It is also shown that as the thermal conductivity parameter increases the fluid velocity and the fluid temperature increases. Also it is observed that neglecting the viscosity and thermal conductivity variation will give substantial errors.

The aim of the present study is to numerically investigate the effect of angle inclination on the natural convection from heated inclined plate with variable viscosity and thermal conductivity.

2. Problem description:

Consider a two-dimensional, steady state flow of viscous incompressible fluid past a semi-infinite heated plate, which inclined at an angle θ to the vertical axis at constant temperature. The x-axis is taken along the plate and the y-axis is perpendicular to the plate at the leading edge, as shown in fig (1). The gravitational acceleration (g) is acting down ward. The plate temperature is assumed to be T_ω and the surrounding stationary fluid temperature is T_∞ . All physical properties are assumed to be constant except for the thermal conductivity, which varies linearly with the fluid temperature and the fluid viscosity which varies exponentially with the fluid temperature.

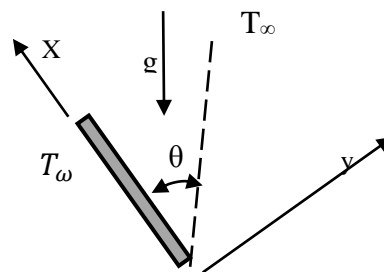


Fig (1) The physical coordinate

3. Mathematical and numerical formulation:

For steady state, two-dimensional, incompressible fluids with Boussinesq approximation, the governing equations are given by [9,10]:

Continuity equation:

$$u \frac{\partial u}{\partial x} + v \frac{\partial v}{\partial y} = 0 \quad (1)$$

x-momentum equation:

$$u \frac{\partial u}{\partial x} + v \frac{\partial u}{\partial y} = -\frac{1}{\rho} \frac{\partial p}{\partial x} + \frac{1}{\rho} \frac{\partial}{\partial x} \left(\mu \frac{\partial u}{\partial x} \right) + \frac{1}{\rho} \frac{\partial}{\partial y} \left(\mu \frac{\partial u}{\partial y} \right) + g\beta(t - T_\infty) \cos\theta \quad (2)$$

y-momentum equation:

$$u \frac{\partial v}{\partial x} + v \frac{\partial v}{\partial y} = -\frac{1}{\rho} \frac{\partial p}{\partial y} + \frac{1}{\rho} \frac{\partial}{\partial x} \left(\mu \frac{\partial v}{\partial x} \right) + \frac{1}{\rho} \frac{\partial}{\partial y} \left(\mu \frac{\partial v}{\partial y} \right) + g\beta(t - T_\infty) \sin\theta \quad (3)$$

Energy equation

$$u \frac{\partial t}{\partial x} + v \frac{\partial t}{\partial y} = \frac{1}{\rho C_p} \left[\frac{\partial}{\partial x} \left(k \frac{\partial t}{\partial x} \right) + \frac{\partial}{\partial y} \left(k \frac{\partial t}{\partial y} \right) \right] \quad (4)$$

The boundary conditions are

$$\begin{aligned} \text{at } y = 0 \quad u = v = 0 \quad t = T_\omega \\ \text{at } y \rightarrow \infty \quad u \rightarrow 0 \quad p \rightarrow 0 \quad t = T_\infty \end{aligned} \quad (5)$$

Introducing the following non-dimensional quantities:

$$\begin{aligned} X = \frac{x}{L}, Y = \frac{yGr^{1/4}}{L}, U = \frac{uLGr^{-1/2}}{\vartheta}, V = \frac{vLGr^{-1/4}}{\vartheta} \\ Gr = \frac{g\beta L^3(T_\omega - T_\infty)}{\vartheta^2}, T = \frac{t - T_\infty}{T_\omega - T_\infty}, P = \frac{L}{\rho} [p + Lg\rho(x\cos\theta + y\sin\theta)] \quad (6) \\ Pr = \frac{\mu_\circ c_p}{k_\circ}, \vartheta = \frac{\mu_\circ}{\rho} \end{aligned}$$

The variations of thermal conductivity and viscosity with dimensionless temperature T are proposed in the following forms by G.Palani et al [10]:

$$\frac{k}{k_\circ} = (1 + \gamma T) \quad (7)$$

$$\frac{\mu}{\mu_\circ} = e^{-\lambda T} \quad (8)$$

Where γ and λ are the thermal conductivity and viscosity variation parameters, respectively, depending on the nature of fluid. In the present study air is selected as the working fluid with the following ranges [10]:

$$-0.7 \leq \lambda \leq 0, \quad 0 \leq \gamma \leq 6, \quad Pr=0.733$$

Substituting the non-dimensional quantities into Equations (1-4), will be produce the following forms:

Continuity equation

$$\frac{\partial U}{\partial X} + \frac{\partial V}{\partial Y} = 0 \quad (9)$$

Momentum equation

$$\begin{aligned} U \frac{\partial U}{\partial X} + V \frac{\partial U}{\partial Y} = -\frac{L^3}{\mu_\circ^2 Gr} \frac{\partial P}{\partial X} + \frac{\vartheta^2}{Gr^{-1/2} L^3} \left[e^{-\lambda T} \frac{\partial^2 U}{\partial X^2} - \lambda e^{-\lambda T} \left(\frac{\partial T}{\partial X} \right) \left(\frac{\partial U}{\partial X} \right) \right] \\ + \frac{\vartheta^2}{Gr L^3} \left[e^{-\lambda T} \frac{\partial^2 U}{\partial Y^2} - \lambda e^{-\lambda T} \left(\frac{\partial T}{\partial Y} \right) \left(\frac{\partial U}{\partial Y} \right) \right] + T \cos\theta \end{aligned} \quad (10)$$

$$\begin{aligned} U \frac{\partial V}{\partial X} + V \frac{\partial V}{\partial Y} = -\frac{L^3}{\mu_\circ^2 Gr^{-1/2}} \frac{\partial P}{\partial Y} + \frac{\vartheta^2}{Gr^{1/2}} \left[e^{-\lambda T} \frac{\partial^2 V}{\partial X^2} - \lambda e^{-\lambda T} \left(\frac{\partial T}{\partial X} \right) \left(\frac{\partial V}{\partial X} \right) \right] \\ + \left[e^{-\lambda T} \frac{\partial^2 V}{\partial Y^2} - \lambda e^{-\lambda T} \left(\frac{\partial T}{\partial Y} \right) \left(\frac{\partial V}{\partial Y} \right) \right] + T \sin\theta Gr^{1/4} \end{aligned} \quad (11)$$

Energy equation

$$U \frac{\partial T}{\partial X} + V \frac{\partial T}{\partial Y} = \frac{1}{PrGr^{1/2}} \left[((1 + \gamma T) \frac{\partial^2 T}{\partial X^2} + \gamma \left(\frac{\partial T}{\partial X} \right)^2) + ((1 + \gamma T) \frac{\partial^2 T}{\partial Y^2} + \gamma \left(\frac{\partial T}{\partial Y} \right)^2) \right] \quad (12)$$

The corresponding boundary conditions in non-dimensional form are

$$\begin{aligned} U = V = 0 \quad T = T_\omega \quad \text{at} \quad Y = 0 \\ U \rightarrow 0 \quad P \rightarrow 0 \quad T = T_\infty \quad \text{at} \quad Y \rightarrow \infty \end{aligned} \quad (13)$$

The important parameters to be calculated are shear stress and the rate of heat transfer at the plate.

The local shear stress at the plate is defined by [9,10]:

$$\tau_x = \left(\mu \frac{\partial u}{\partial y} \right)_{y=0} \quad (14)$$

By substituting the non-dimensional quantities in Eq. (14), the non-dimensional form of the local skin friction will be

$$C_{fx} = e^{-\lambda Gr^{3/4}} \left(\frac{\partial U}{\partial Y} \right)_{Y=0} \quad (15)$$

The integration of Eq.(15) from X=0 to X=1 gives the average skin friction and it is given by :

$$\bar{C}_f = e^{-\lambda Gr^{3/4}} \int_0^1 \left(\frac{\partial U}{\partial Y} \right)_{Y=0} dX \quad (16)$$

The local Nusselt number is defined by [9,10]:

$$N_{ux} = \frac{-L \left(\frac{\partial t}{\partial y} \right)_{y=0}}{k_o(T_\omega - T_\infty)} \quad (17)$$

By substituting the non-dimensional quantities in Eq. (17), the non-dimensional form of local Nusselt number is given by :

$$N_{ux} = -(1 + \gamma) \left(\frac{\partial T}{\partial Y} \right)_{Y=0} \quad (18)$$

The integration of Eq.(18) from X=0 to X=1 gives the average Nusselt number and it is given by :

$$\bar{N}_u = -(1 + \gamma) \int_0^1 \left(\frac{\partial T}{\partial Y} \right)_{Y=0} dX \quad (19)$$

The governing continuity, momentum and energy equations (9-12) with boundary conditions are solved simultaneously by using a finite volume method. Steady

segregated solver was used with second order upwinding scheme for convective terms in the momentum and energy equation. For pressure-velocity coupling, pressure implicit with splitting of operators (PISO) scheme was used. A convergence criterion of 1×10^{-6} was applied to the residual of the continuity and the momentum equations and 1×10^{-9} to the residual of the energy equation.

4. Results and discussion:

4.1. Validation

In order to check the accuracy of the present work, a comparison is made with [10]. A comparison of velocity and temperature profiles at $X=1$ for steady state. The comparison is done for air with $Pr=0.733$ of vertical plate ($\theta = 0$) and $\lambda=-0.4$ with $\gamma=(0, 2, 4)$. Fig (2) shows the variation of U from [10] with U obtained from the present work with Y for $\lambda=-0.4$ and $\gamma=(0, 2, 4)$. From this figure it can be seen that, the agreement is acceptable and the average error is 1.7%. The variation of T from [10] with T obtained from the present work with Y for $\lambda=-0.4$ and $\gamma=(0, 2, 4)$ is shown in Fig (3). From this figure the average error is 2% and the agreement is acceptable. From these figures, it can be concluded that the present model has good accuracy and can be used accurately.

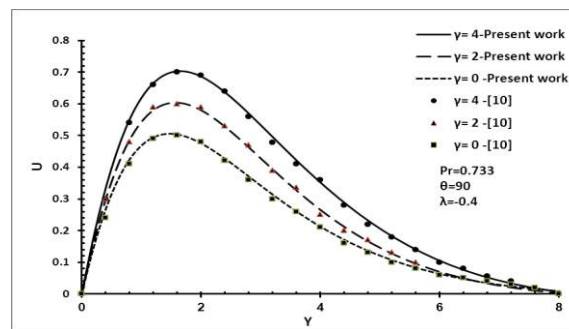


Fig (2) Variation of U with Y for $\lambda=-0.4$ and $\gamma=(0, 2, 4)$ as comparison between data of [10] and result of present

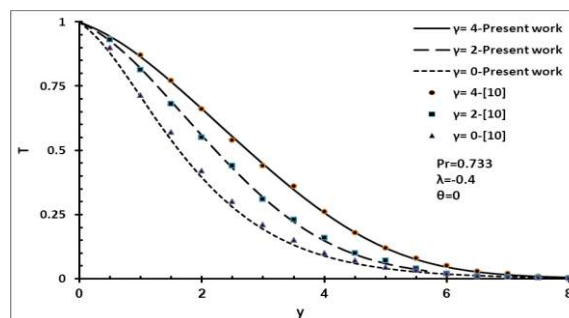


Fig (3) Variation of T with Y for $\lambda=-0.4$ and $\gamma=(0, 2, 4)$ as comparison between data of [10] and result of present

To study the effect of inclination angle on the behavior of the local skin friction and local Nusselt number of natural convection from inclined plate for variable thermal conductivity and viscosity. Fig (4-a) shows the variation of local skin friction with X for $\theta=0$, $Pr=0.733$ and $\lambda=-0.2$ with different value of γ , It can be seen that the local skin friction increases as X increase due to increase velocity of air from the leading edge to the rear of the plate. The effects of increasing the thermal conductivity parameter γ on the local skin friction are as the γ increase, the local skin friction increase due to increase of thermal conductivity of air that cases an incensement in the velocity of air near the plate. The increment of local skin friction is different according to the location of X on the plate therefor three point are chosen on the plate $X=0.25$, $X=0.5$ and $X=0.75$ to explain increment percentage .The increment percentage are listed in table (1). Fig (4-b) present the variation of local skin friction with X for $\theta=0$, $Pr=0.733$ and $\gamma=2$ with different value of λ , It can observed that the local skin friction increases as X increase due to increase velocity of air from the leading edge to the rear of the plate. The effects of decreasing the viscous variation parameters λ , on the local skin friction are as the λ decrease, the local skin friction increase due to increase the velocity of air caused by decreasing the viscosity of air. The increment percentages are listed in table (1).

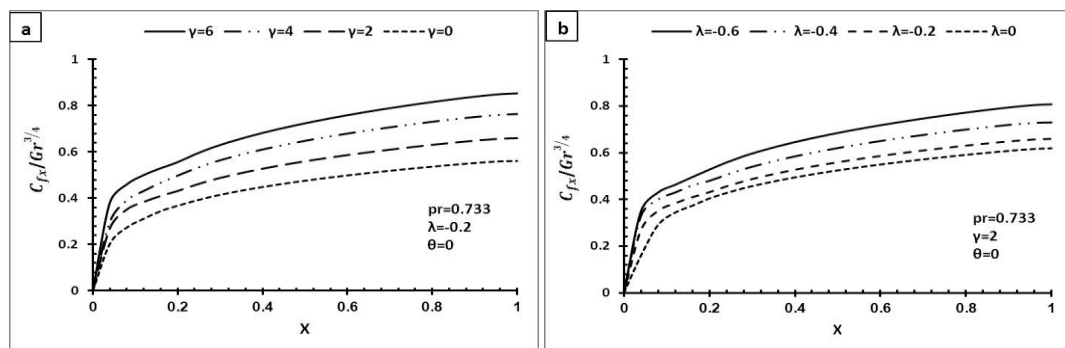


Fig (4) Variation of local skin friction with X for $\theta=0$ (a) $\lambda= -0.2$ and different γ , (b) $\gamma =2$ and different λ .

Fig (5-a) illustrate the variation of local Nusselt number with X for $\theta=0$, $Pr=0.733$ and $\lambda= -0.2$ and different value of γ . From this figure it can be seen that the local Nusselt number begin with the greatest value at the beginning of the plate then suffer from a sharp decline until $X=0.08$ after that it decrease gradually to the end of the plate. This behavior is due to increase thermal boundary layer thickness as it proceed from the leading edge to the rear of the plate, with corresponding smaller wall temperature gradient and hence smaller local Nusselt number. The effects of increasing the thermal conductivity parameter γ on the local Nusselt number are as the γ increase,

the local Nusselt number increases for the same value of X due to increasing thermal conductivity that result in increased temperature of air. The increment percentages are listed in table (2). Fig (5-b) present the variation of local Nusselt number with X for $\theta=0$, $Pr=0.733$ and $\gamma=2$ with different value of λ , It can observed that the local Nusselt number behave in the same way in as in fig (5-a). The effects of decreasing the viscous variation parameters λ , on the local Nusselt number are as the λ decrease, the local Nusselt number decrease due to decreasing the viscosity of air casing lower temperature of air near the plate. The increment percentages are listed in table (2).

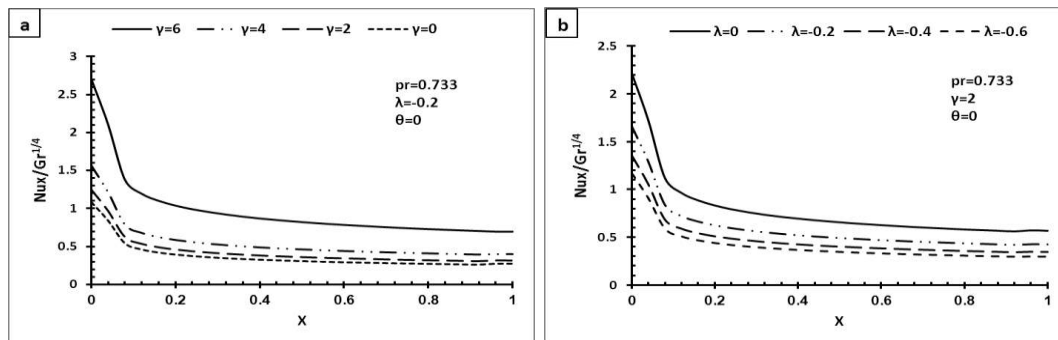


Fig (5) Variation of local Nusselt number with X for $\theta=0$ (a) $\lambda=-0.2$ and different γ , (b) $\gamma=2$ and different λ .

Fig (6-a) represent the variation of local skin friction with X for $\theta=30$, $Pr=0.733$ and $\lambda=-0.2$ with different value of γ . It can be seen that the local skin friction increase from the beginning of the plate to $X=0.04$ then it suffer from a slight decrease to $X=0.16$ then it begins to increase until it arrives at the greatest value at $X=0.84$ and then fall to the end of the plate. This behavior is a result of generation of vortexes and disturbance of boundary layer in the regain of the leading and the rear edges due to increase angle of inclination. The effects of increasing the thermal conductivity parameter γ on the local skin friction is Similar to that in Fig (4-a). The increment percentages are listed in table (1). From Fig (6-b) It can be seen that the local skin friction behave in the same way as in Fig (6-a) but for $\theta=30$, $Pr=0.733$ and $\gamma=2$ and different value of λ . The effects of decreasing the viscous variation parameters λ , on the local skin friction are similar to that in Fig (4-b). The increment percentages are listed in table (1).

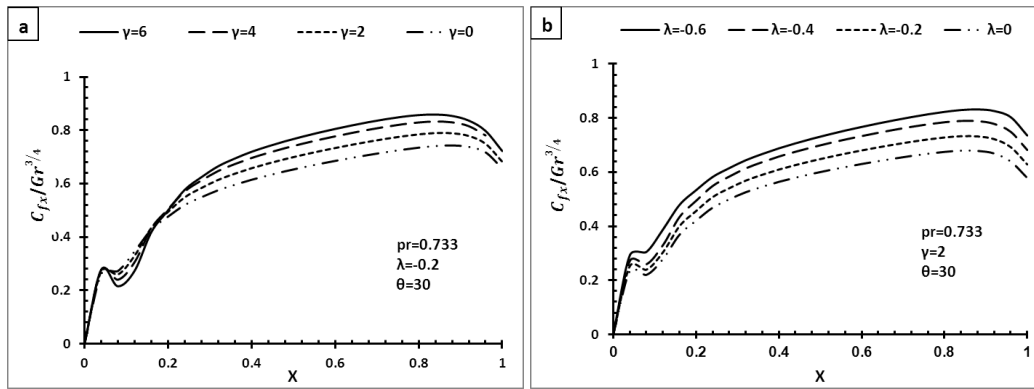


Fig (6) Variation of local skin friction with X for $\theta=30$ (a) $\lambda= -0.2$ and different γ , (b) $\gamma =2$ and different λ .

Fig (7-a) shows variation of local Nusselt number with X for $\theta=30$, $Pr=0.733$ and $\lambda= -0.2$ with different value of γ . It can be seen that local Nusselt number behave in the same way of fig (5-a) except for the rear of the plate it Increase to the end of the plate. The Incensement of local Nusselt number in the rear of the plate is due to generation of vortex in the rear of the plate that result in larger wall temperature gradient hence a larger local Nusselt number. The effects of increasing the thermal conductivity parameter γ on the local Nusselt number are similar to that in fig (5-a). The increment percentages are listed in table (2). Fig (7-b) present the variation of local Nusselt number with X for $\theta=30$, $Pr=0.733$ and $\gamma= 2$ with different value of λ , It can observed that the local Nusselt number behave in same way as in fig (7-a). The effects of decreasing the viscous variation parameters λ on the local Nusselt number are as the λ decrease, the local Nusselt number decrease due to decreasing the viscosity of air casing lower temperature of air near the plate. The increment percentages are listed in table (2).

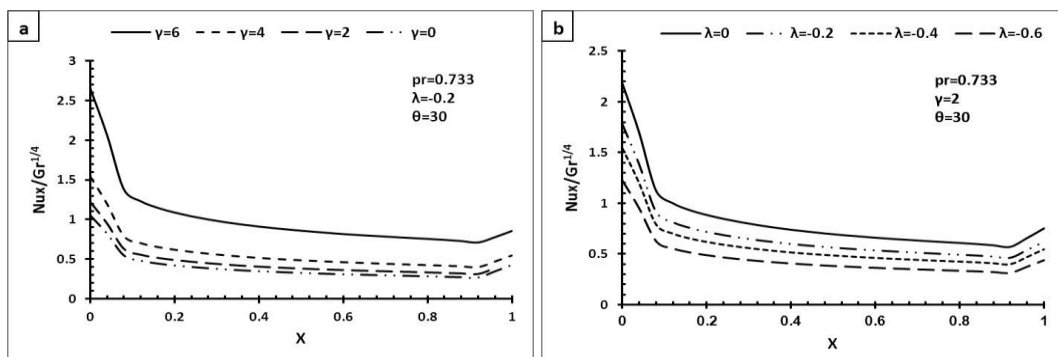


Fig (7) Variation of local Nusselt number with X for $\theta=30$ (a) $\lambda= -0.2$ and different γ , (b) $\gamma =2$ and different λ .

Fig (8-a) show the variation of local skin friction with X for $\theta=60$, $Pr=0.733$ and $\lambda=-0.2$ with different value of γ , It can be seen that the local skin friction increase from the beginning of the plate to $X=0.04$ then it suffer from a decline between $X=0.05$ to $X=0.12$ then it increase until it reaches maximum value at $X= 0.76$ after this point it decrease to the end of the plate. This trend is expected because larger angle of inclination results in generation of vortex in the regain between $X=0.05$ to $X=0.12$ and the rear of the plate, that effect on the boundary layer in that regain decreasing the velocity of air near the plate and hence lower local skin friction. The effects of increasing the thermal conductivity parameter γ on the local skin friction is Similar to that in Fig (4-a). The increment percentages are listed in table (1). From Fig (8-b) It can be seen that the local skin friction behave in the same way as in Fig (8-a) but for $\theta=60$, $Pr=0.733$ and $\gamma =2$ and different value of λ . The effects of decreasing the viscous variation parameters λ , on the local skin friction are similar to that in Fig (4-b). The increment percentages are listed in table (1).

Fig (9-a) shows variation of local Nusselt number with X for $\theta=60$, $Pr=0.733$ and $\lambda= -0.2$ with different value of γ . It can be seen that the local Nusselt number begin with the maximum value then suffer from a severe decline until $X=0.07$ after that it decrease gradually until $X=0.9$ then increase to end of the plate. This behavior is due to increase the angle of inclination that result in increased thermal boundary layer thickness as it proceed from the leading edge to the rear of the plate, with generation of vortex in the leading and rear edge of the plate that produced smaller wall temperature gradient and hence smaller local Nusselt number. The effects of increasing the thermal conductivity parameter γ on the local Nusselt number are similar to that in fig (5-a). The increment percentages are listed in table (2). Fig (9-b) shows the variation of local Nusselt number with X for $\theta=60$, $Pr=0.733$ and $\gamma= 2$ with different value of λ , It can observed that the local Nusselt number conduct analogous to fig (9-a). The effects of decreasing the viscous variation parameters λ , on the local Nusselt number are similar to fig (5-b). The increment percentages are listed in table (2)

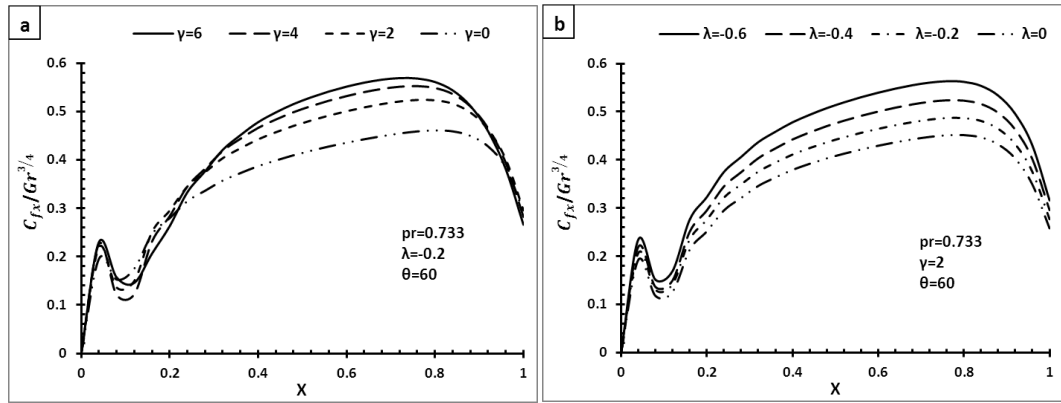


Fig (8) Variation of local skin friction with X for $\theta=60$ (a) $\lambda= -0.2$ and different γ , (b) $\gamma =2$ and different λ .

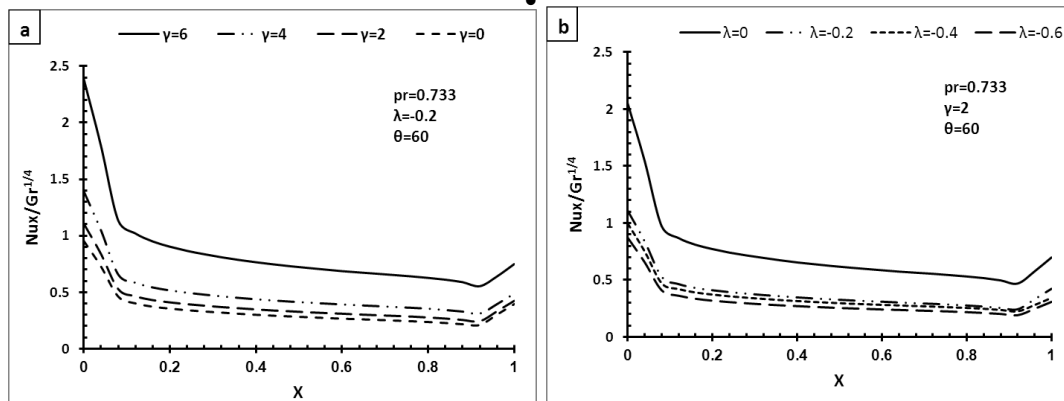


Fig (9) Variation of local Nusselt number with X for $\theta=60$ (a) $\lambda= -0.2$ and different γ , (b) $\gamma =2$ and different λ .

The variation of local skin friction with X for $\theta=90$, $Pr=0.733$ and $\lambda= -0.2$ at different values of γ is presented in fig (10-a). From this figure It can be observed that, The local skin friction increased from the beginning of the plate to $X=0.06$ after that it has sharp decline until $X=0.1$ then it increases gradually to $X=0.24$ then the local skin friction decrease until it reach the minimum value at the center of the plate. The local skin friction repeats the same variation along the second half of the plate in inverse pattern. This is due to the horizontal position of the plate that produce movement of cooled air from the side towards the center of the plate result in increased the local skin friction from the beginning of the plate to $X=0.06$. After that due to increase the temperature and decreasing the density of air case to move the air in vertical direction. This decrease the air velocity component parallel to the plate when moving towards the center of the plate hence decreases the local skin friction. The effects of increasing the thermal conductivity parameter γ on the local skin friction is Similar to that in Fig (4-a). The increment percentages are listed in table (1). In fig (10-b) It can be seen that the local skin friction behave in the same way as in Fig (10-a) but for $\theta=90$, $Pr=0.733$ and $\gamma =2$ and different value of λ . The effects of decreasing the viscous variation

parameters λ , on the local skin friction are similar to that in Fig (4-b). The increment percentages are listed in table (1).

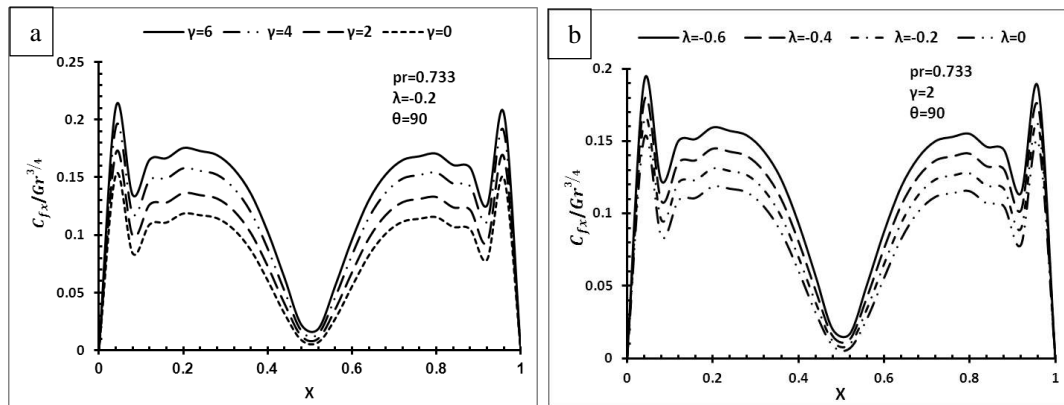


Fig (10) Variation of local skin friction with X for $\theta=90$ and (a) $\lambda= -0.2$ and different γ , (b) $\gamma=2$ and different λ .

Fig (11-a) present the variation of local Nusselt number with X for $\theta=90$, $Pr=0.733$ and $\lambda= -0.2$ with different value of γ . From this figure it can be observed that the local Nusselt number begin with greatest value at the sides of the plate then it decreases sharply in the leading edges. After that it decreases gradually until it reaches the lowest value at the center of the plate. This behaves is due to the temperature difference between the plate and the air is at the maximum value at the sides of the plate then due to increase of air temperature that moves toward the center of the plate result in decrease the local Nusselt number. The effects of increasing the thermal conductivity parameter γ on the local Nusselt number are similar to that in fig (5-a). The increment percentages are listed in table (2) . Fig (11-b) shows the variation of local Nusselt number with X for $\theta=90$, $Pr=0.733$ and $\gamma= 2$ with different value of λ , It can observed that the local Nusselt number conduct analogous to fig (9-a). The effects of decreasing the viscous variation parameters λ , on the local Nusselt number are similar to fig (5-b). The increment percentages are listed in table (2).

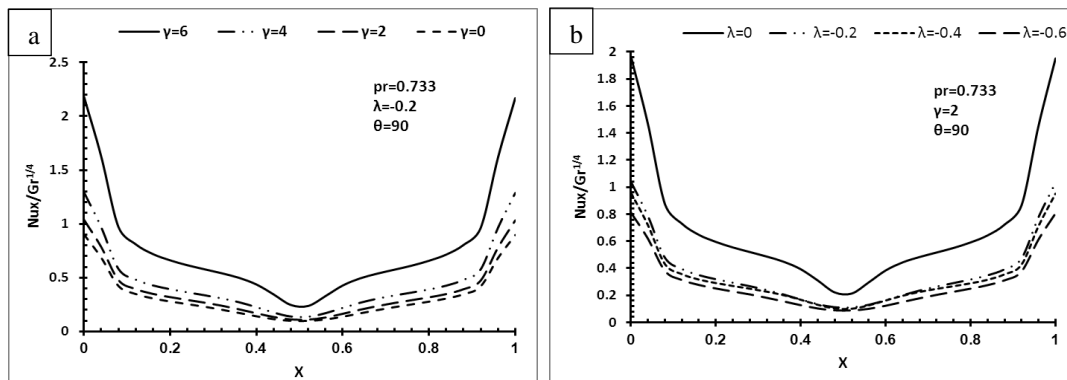


Fig (11) Variation of local Nusselt number with X for $\theta=90$ (a) $\lambda= -0.2$ and different γ , (b) $\gamma=2$ and different λ .

Table (1) Increment percentages of local skin friction for different angle and γ , λ parameters.

θ	Increment percentage of local skin friction for $\lambda = -0.2$ and $Pr = 0.733$ with different γ				Increment percentage of local skin friction for $\gamma = 2$ and $Pr = 0.733$ with different λ			
		X=0.2 5	X=0.5	X=0.7 5		X=0.2 5	X=0.5	X=0.75
0	from $\gamma = 0$ to $\gamma = 2$	17.1 %	18.9 %	17.5 %	from $\lambda = 0$ to $\lambda = -0.2$	6.7%	6.8%	6.6%
	from $\gamma = 2$ to $\gamma = 4$	15.5 %	15.7 %	15.9 %	from $\lambda = -0.2$ to $\lambda = -0.4$	9.7%	10.7 %	9.4%
	from $\gamma = 4$ to $\gamma = 6$	11.5 %	11.7 %	11.6 %	from $\lambda = -0.4$ to $\lambda = -0.6$	10.4 %	10.5 %	11.8%
3	from $\gamma = 0$ to $\gamma = 2$	5.5%	7.1%	6.8%	from $\lambda = 0$ to $\lambda = -0.2$	8.3%	8%	7.7%
	from $\gamma = 2$ to $\gamma = 4$	4%	5.9%	5.9%	from $\lambda = -0.2$ to $\lambda = -0.4$	8%	7.7%	7.7%
	from $\gamma = 4$ to $\gamma = 6$	1%	3.6%	3.4%	from $\lambda = -0.4$ to $\lambda = -0.6$	6%	4.6%	4.7%
60	from $\gamma = 0$ to $\gamma = 2$	9.5%	15%	14.1 %	from $\lambda = 0$ to $\lambda = -0.2$	8.8%	8.2%	7.7%
	from $\gamma = 2$ to $\gamma = 4$	2.9%	6.2%	5.2%	from $\lambda = -0.2$ to $\lambda = -0.4$	7.1%	7.8%	7.6%
	from $\gamma = 4$ to $\gamma = 6$	3.4%	3.5%	2.8%	from $\lambda = -0.4$ to $\lambda = -0.6$	9%	7.9%	7.4%
9	from $\gamma = 0$ to $\gamma = 2$	14.5 %	4.3%	14.5 %	from $\lambda = 0$ to $\lambda = -0.2$	10.2 %	3.8%	10.2%
	from $\gamma = 2$ to $\gamma = 4$	15.6 %	3.8%	15.6 %	from $\lambda = -0.2$ to $\lambda = -0.4$	10%	3.1%	10%
	from $\gamma = 4$ to $\gamma = 6$	10.9 %	3.3%	10.9	from $\lambda = -0.4$ to $\lambda = -0.6$	10.5 %	2.9%	10.5%

Table (2) Increment percentages of local Nusselt number for different angle and γ, λ parameters.

θ	Increment percentage of local Nusselt number for $\lambda = -0.2$ and $Pr = 0.733$ with different γ				Increment percentage of local Nusselt number for $\gamma = 2$ and $Pr = 0.733$ with different λ			
		X=0.2 5	X=0.5	X=0.7 5		X=0.2 5	X=0.5	X=0.75
0	from $\gamma = 0$ to $\gamma = 2$	16.8 %	17%	16.9 %	from $\lambda = -0.6$ to $\lambda = -0.4$	15.9 %	15.7 %	15.8%
	from $\gamma = 2$ to $\gamma = 4$	27.6 %	28.2 %	28.3 %	from $\lambda = -0.4$ to $\lambda = -0.2$	22.3 %	22.4 %	22.7%
	from $\gamma = 4$ to $\gamma = 6$	77.2 %	77.5 %	77.5 %	from $\lambda = -0.2$ to $\lambda = 0$	33.5 %	33.6 %	33.2%
30	from $\gamma = 0$ to $\gamma = 2$	16.4 %	16.7 %	17.3 %	from $\lambda = -0.6$ to $\lambda = -0.4$	26.8 %	26.9 %	27.1%
	from $\gamma = 2$ to $\gamma = 4$	26.5 %	27.6 %	27.5 %	from $\lambda = -0.4$ to $\lambda = -0.2$	16% %	16% %	16%
	from $\gamma = 4$ to $\gamma = 6$	75.9 %	76.8 %	77.9 %	from $\lambda = -0.2$ to $\lambda = 0$	23.3 %	23.3 %	23.6%
60	from $\gamma = 0$ to $\gamma = 2$	15.5 %	15.8 %	16.8 %	from $\lambda = -0.6$ to $\lambda = -0.4$	17% %	16.7 %	16.5%
	from $\gamma = 2$ to $\gamma = 4$	25.9 %	26.3 %	27.4 %	from $\lambda = -0.4$ to $\lambda = -0.2$	10% %	9.8% %	9.2%
	from $\gamma = 4$ to $\gamma = 6$	74.7 %	75.4 %	76.7 %	from $\lambda = -0.2$ to $\lambda = 0$	88.2 %	89.4 %	91.1%
90	from $\gamma = 0$ to $\gamma = 2$	15.8 %	12.2 %	15.8 %	from $\lambda = -0.6$ to $\lambda = -0.4$	17.9 %	13.6 %	17.9%
	from $\gamma = 2$ to $\gamma = 4$	23.8 %	23.6 %	23.8 %	from $\lambda = -0.4$ to $\lambda = -0.2$	8.9% %	10% %	8.9%
	from $\gamma = 4$ to $\gamma = 6$	69.4 %	74.2 %	69.4 %	from $\lambda = -0.2$ to $\lambda = 0$	81.9 %	93.3 %	81.9%

Fig (12) illustrate the variation of average skin friction with θ for $Pr = 0.733$ and $\lambda = -0.4$ with different values of γ . It can be seen that the average skin friction decreased with increase θ due to decrease the velocity tangent to the plate. Also it can be seen that the average skin friction increase with increase the value of the thermal conductivity parameter γ for all values of θ . The maximum increment percentage is at $\theta = 0$, from $\gamma = 0$ to $\gamma = 2$ is 11.1%, from $\gamma = 2$ to $\gamma = 4$ is 4.3% and from $\gamma = 4$ to $\gamma = 6$ is 3.7%.

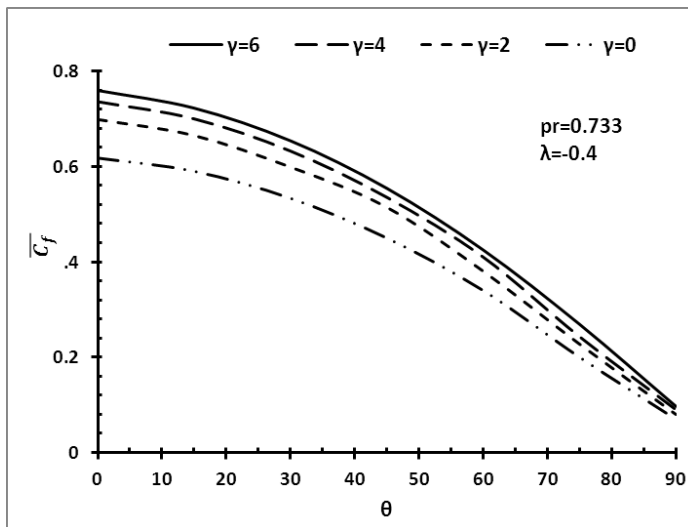


Fig (12) Variation of average skin friction with θ for $Pr=0.733$ and $\lambda=-0.4$ with different γ .

Fig (13) shows variation of average Nusselt number with θ for $Pr=0.733$ and $\gamma=4$ with different λ . It can be seen that the average Nusselt number decrease as θ increase. The effects of decreasing the viscous variation parameters λ , on the average Nusselt number are as the λ decrease, the average Nusselt number decrease for the same value of θ . The maximum increment percentage is at $\theta=0$, from $\lambda =-0.6$ to $\lambda =-0.4$ is 8.8 %, from $\lambda =-0.4$ to $\lambda =-0.2$ is 8.1% and from $\lambda =-0.2$ to $\lambda =0$ is 8 %.

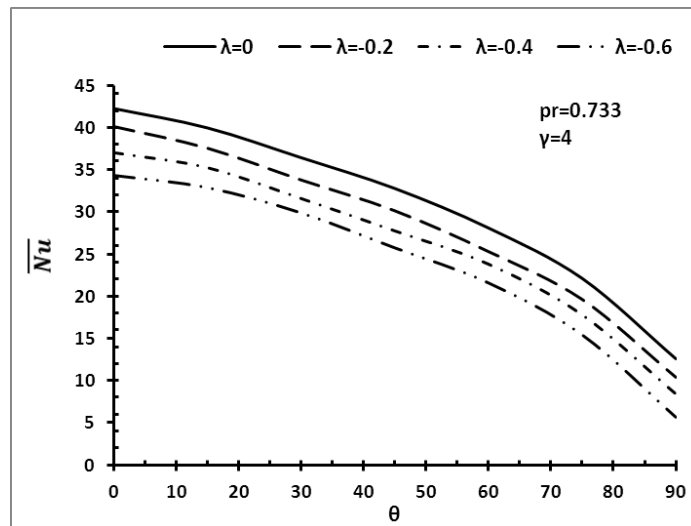


Fig (13) Variation of average Nusselt number with θ for $Pr=0.733$ and $\gamma=4$ with different λ .

5- Conclusions

In this paper, the effect of inclination angle on natural convection from inclined plate with variable viscosity and thermal conductivity has been studied. From the results obtained, the following conclusions can be drawn:

- 1- The distribution of local skin friction on the inclined plate is effected by the inclination angle.
- 2- The distribution of local Nusselt number on the inclined plate is effected by the inclination angle.
- 3- The local skin friction increase with increasing the thermal conductivity parameter γ also it increase with decrease the viscous variation parameters λ . the maximum increment for the two cases at $\theta=0$.
- 4- The Nusselt number increase with increasing the thermal conductivity parameter γ while it decrease with deceasing the viscous variation parameters λ . the maximum increment for the two cases at $\theta=0$.
- 5- The average skin friction decreased with increasing θ .
- 6- The average Nusselt number decreased with increasing θ .

6-References

- [1] Michiyoshi,I.,1964,"Heat Transfer from an Inclined Thin Flat Plate by Natural Convection", The Japan Society of Mechanical Engineering, Vol.7, No.28,pp. 745-759.
- [2] H. -T. Lin, C. -M. Wu,1997,"Combined heat and mass transfer by laminar natural convection from a vertical plate with uniform heat flux and concentration", Heat and Mass Transfer , Vol.32 ,PP. 293–299.
- [3] Onur, N., Sivrioglu, M., Aktas, M.K., 1997," An experimental study on the natural convection heat transfer between inclined plates (Lower plate isothermally heated and the upper plate thermally insulated as well as unheated)", Heat and Mass Transfer, Vol.32, pp. 471-476.
- [4] P. Ganesan, G. Palani, 2003," Natural convection effects on impulsively started inclined plate with heat and mass transfer", Heat and Mass Transfer, Vol. 39, pp. 277–283.
- [5] Dias, Jr.T. , Milanez, L.F.,2004, "Natural convection due to a heat source on a vertical plate ", International Journal of Heat and Mass transfer , Vol.47,pp. 1227-1232.
- [6] Yao, L.S., 2006," Natural convection along a vertical complex wavy surface", International Journal of Heat and Mass transfer, Vol.49, pp. 281-286.

- [7] Mahanti, N.C., Gaur, P., 2009,"Effects of Varying Viscosity and Thermal Conductivity on Steady Free Convective Flow and Heat Transfer Along an Isothermal Vertical Plate in the Presence of Heat Sink", Journal of Applied Fluid Mechanics, Vol. 2, No. 1, pp. 23-28.
- [8] Saha, S.C., Patterson, J.C., Lei, C., 2010,"Scaling of natural convection of an inclined flat plate: Ramp cooling condition", International Journal of Heat and Mass transfer, Vol.53, pp. 5156-5166.
- [9] Siddiqa, S., Asghar, S., Hossain, M.A., 2010,"Natural convection flow over an inclined flat plate with internal heat generation and variable viscosity", Mathematical and Computer Modeling, Vol. 52, pp. 1739-1751.
- [10] Palani, G., Kim, K.Y., 2010, "Numerical study on a vertical plate with variable viscosity and thermal conductivity", Arch Apple Mach, Vol. 80, pp. 711–725.

7-Nomenclature

Symbol	Description	Units
\bar{C}_f	average skin friction	
\bar{N}_u	average Nusselt number	
C_{fx}	local skin friction	
C_p	specific heat	J kg ⁻¹ K ⁻¹
N_{ux}	local Nusselt number	
k_o	thermal conductivity at plate temperature	W m ⁻¹ K ⁻¹
μ_o	viscosity at plate temperature	Kg m ⁻¹ s ⁻¹
τ_x	local shear stress at the plate	
G	acceleration due to gravity	m s ⁻²
Gr	Grashof number	
L	length of the plate	m
P	Fluid pressure	Pa
Pr	Prandtl number	
T	temperature of the fluid	K ^o
T	Dimensionless fluid temperature	
T _∞	surrounding stationary fluid temperature	K ^o
T _ω	plate temperature	K ^o
Γ	thermal conductivity variation parameter	
Θ	Angle of inclination of the plate to the vertical	Degree
Λ	viscosity variation parameter	
U	Dimensionless fluid velocity in x direction	
V	Dimensionless fluid velocity in y direction	
X	Dimensionless Cartesian Coordinates in x direction	
Y	Dimensionless Cartesian Coordinates in x direction	
k	variable thermal conductivity of the fluid	W m ⁻¹ K ⁻¹
u	Dimensional fluid velocity in x direction	m s ⁻¹
v	Dimensional fluid velocity in y direction	m s ⁻¹
β	coefficient of volume expansion	1/K ^o
μ	variable dynamic coefficient of viscosity	Kg m ⁻¹ s ⁻¹
ρ	density of the fluid	Kg m ⁻³
ν	kinematic viscosity	m ² s ⁻¹